



# Transmission of $^{155}\text{Eu}$ lines: a quick method to create efficiencies for gamma spectroscopy estimating sample self-absorption at low energy

Manuel Pérez-Mayo<sup>1</sup> · Helmut W. Fischer<sup>1</sup>

Received: 31 May 2018 / Published online: 16 August 2018  
© Akadémiai Kiadó, Budapest, Hungary 2018

## Abstract

A method is presented to obtain efficiency calibration for samples of unknown composition in gamma spectrometry. It is based on photon transmission measurements using  $^{155}\text{Eu}$ , a multi-energetic gamma emitter. An iterative algorithm produces a virtual chemical composition reproducing the measured sample self-absorption in the range 43–146 keV. The composition is then used to numerically create a sample-specific efficiency calibration. The procedure was tested with IAEA certified sediment materials containing  $^{210}\text{Pb}$ ,  $^{241}\text{Am}$ ,  $^{155}\text{Eu}$ , and  $^{226}\text{Ra}$ . The deviation from certified values ranged between 3 and 22%, within the range of experimental uncertainty (between 5 and 35%, due to low isotope concentrations).

**Keywords** Gamma spectrometry · Efficiency calibration · Self-absorption · Chemical composition ·  $^{155}\text{Eu}$

## Introduction

In environmental sciences, determination of natural and man-made radioisotopes is an important tool to understand environmental systems. Radioisotopes as  $^{210}\text{Pb}$ ,  $^{226}\text{Ra}$ ,  $^{137}\text{Cs}$ ,  $^{241}\text{Am}$  are commonly used for dating sediments [1–3].  $^7\text{Be}$  has been used for atmospheric studies and  $^{232}\text{Th}$  or  $^{238}\text{U}$  series give us important information for understanding soils or sediments. All of them have been measured widely with gamma spectrometry [4, 5]. It makes gamma spectrometry a powerful tool with the advantages of being easy, fast and multi-elemental but with some well known disadvantages. When low energy gamma emitters are present in the sample such as  $^{210}\text{Pb}$  (46.5 keV),  $^{241}\text{Am}$  (59.5 keV) or  $^{232}\text{Th}$  (63.8 keV), self-absorption effects become an important problem in the activity determination. Self-absorption is principally governed by: density, chemical composition and size of the sample, bearing the

danger of over- or under-determination of the activities from the cited nuclides [6].

During the last 30 years, this problem has been partially solved with transmission measurement of one nuclide for different sample compositions [7]. The original method was restricted by geometries (sample volume and source-detector geometry), accessibility to standardized solutions and experimental time [7, 8]. Later works based on Monte Carlo codes eliminated the second problem of the geometrical configuration: first using a low energy photon collimated beam [9], and in the later work using a non-collimated one together with Monte Carlo code GEANT 3.21 [10]. Advanced methods [11] permitted to extend the concept from single to a range of energies and different filling heights for a fixed sample container. Despite of solving the problem, methods still have some partial restrictions by geometry “height”, programming self-developed Monte Carlo codes or expertise use of the code GEANT 3–4 widely used in the field. The use of several point sources like  $^{241}\text{Am}$ ,  $^{210}\text{Pb}$ ,  $^{137}\text{Cs}$  or  $^{60}\text{Co}$  for transmission experiments [6, 10] make classical methods laborious to apply.

On the other hand, codes based on Monte Carlo method are widely used to create Full Energy Peak Efficiencies (FEPE) for samples with user-definable geometries, size and sample composition. ISOCS/LabSOCS [12] is one example based on the MCNP (Monte Carlo N-Particle)

**Electronic supplementary material** The online version of this article (<https://doi.org/10.1007/s10967-018-6092-x>) contains supplementary material, which is available to authorized users.

✉ Manuel Pérez-Mayo  
manuel@iup.physik.uni-bremen.de

<sup>1</sup> Institute of Environmental Physics, University of Bremen,  
28359 Bremen, Germany

code. The software can provide FEPE in a range between 10 and 7 MeV for multiple geometry configurations and sample chemical composition [12]. Uncertainty produced in the FEPE calculations are specified by default from the software manufacturer to be  $\pm 15\%$  for energies between 10 and 45 keV,  $\pm 10\%$  for energies between 45 and 150 keV,  $\pm 8\%$  for energies between 150 and 300 keV,  $\pm 6\%$  for energies between 300 and 700 keV and  $\pm 4\%$  for energies between 700 and 2000 keV.

Self-developed Monte Carlo codes or ISOCS/LabSOCS takes into account physical properties of the sample, e.g. chemical composition, density, geometry, etc. Chemical composition of the sample container and geometry can be modeled with accuracy as well. FEPE can be produced whenever information of the last parameters is provided. Nevertheless in sediment samples knowledge of the chemical composition is not always known. For example, an underdetermined percent of  $\text{CaCO}_3$  in the sample changes substantially the calculated activity concentration of  $^{210}\text{Pb}$  due to the self-absorption effect, it means that dating models will be directly affected [13].

Here, we present a method to estimate the self-absorption of a sediment sample with unknown chemical composition. The method tests different virtual chemical compositions and looks for an “effective” composition that produces suitable self-absorption values. Later on, this effective composition is used to obtain FEPE using ISOCS/LabSOCS.

## Theoretical background

In a sample with homogeneous chemical composition, self-absorption of photons ( $\gamma$  and X-rays) inside the sample can be described by the mass attenuation coefficient:  $\mu/\rho$ . This parameter is governed by interaction of photons with matter: photoelectric effect, Compton scattering and pair production. The attenuation of photons depends on  $Z$  of the materials present in the sample and energy of the incoming photon. The total effect can be described approximately by

$$\frac{\mu(E)}{\rho} = \left( C_\tau \frac{Z^{4.5}}{E^3} + C_\sigma \frac{Z}{E} + C_\kappa Z^2 \right) \cdot \frac{N_A}{M} \quad (1)$$

where  $C_\tau$ ,  $C_\sigma$  and  $C_\kappa$  are constants for every effect respectively [14],  $Z$  is the atomic number for a determined material,  $E$  the energy of the incoming photons,  $N_A$  the Avogadro constant and  $M$  the molar mass. The linear attenuation coefficient  $\mu$  can be calculated just by multiplying Eq. (1) by the density. From Eq. (1) can be observed that absorption of low energy photons will depend strongly on  $Z$  present in the sample.

The basis of the proposed method lies on a photon transmission experiment, similar to the work presented in

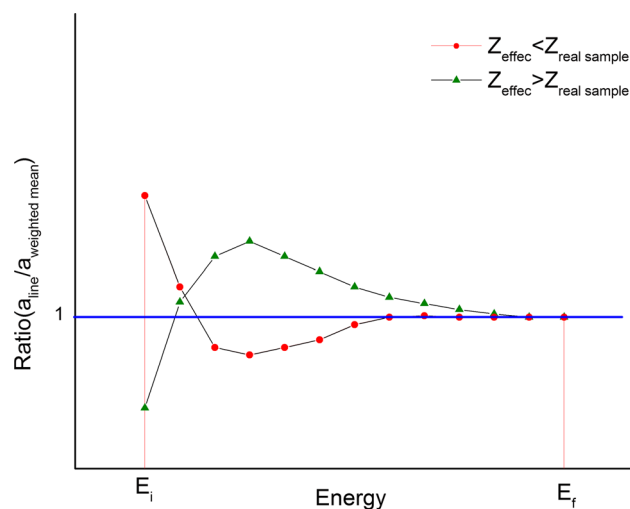
[6], but in our case only one multi-line radioisotope is used:  $^{155}\text{Eu}$ . If the activity of one multi-line element is measured, the same activity must be found for all lines.  $^{155}\text{Eu}$  emits photons with energies between 26.5 and 146.1 keV. The low energy photons are more strongly absorbed than the photon of 146.1 keV in the sample. Plotting individual activity ratios (activity calculated with one line divided by the mean value of the nuclide activity or a fixed key line) an under or over determined  $Z$  can be shown, see Fig. 1.

Assuming an unknown chemical composition, a natural sediment sample can be described chemically by a combination of standard minerals [7], water and an organic material like cellulose, see Table 1.

Considering a configuration source-absorber-detector where a point source is placed 10 cm above detector and one cylindrical slice of sediment wrapped in a layer of container material acting as absorber is placed on the detector, see Fig. 2.

The sediment layer plays the role of absorber with a known geometry and density but with an unknown chemical composition described by a set of five  $w_i$  free parameters. Every component  $w_i$  of the vector  $\mathbf{w}$  represents the components from Table 1. Taking into account the geometrical configuration and an “initial” chemical composition, for example: water 100%, a set of FEPEs for the  $E_k$  lines of  $^{155}\text{Eu}$  is generated using ISOCS/LabSOCS:  $\varepsilon_{\text{ini}}(E_k)$ . FEPE is applied together with the experimental transmission spectra to calculate activities  $A_{\text{ini}_k}$  for individual lines  $E_k$ , see Fig. 2.

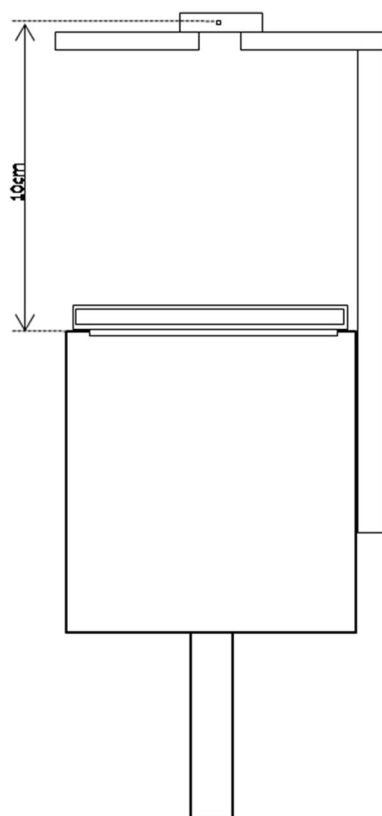
The initial value of the vector  $\mathbf{w}$  (also  $\mathbf{w}_{\text{ini}} = (0,0,0,1,0)$ ), together with initial FEPEs  $\varepsilon_{\text{ini}}(E_k)$  and activities  $A_{\text{ini}_k}$  are introduced into the algorithm. The algorithm calculates a



**Fig. 1** Example of activity ratios in case of a transmission experiment, where only the sample composition is taken into account. Ratios deviation from unity will be expected when the selected effective  $Z$  for the model differs from the mean  $Z$  in the sample

**Table 1** Standard materials used in the model, together with elemental chemical composition in percent of the atom weight and index used in the algorithm

Mineral	Algorithm index <i>i</i>	Composition	Elemental composition
Hematite	1	Fe <sub>2</sub> O <sub>3</sub>	Fe (69.8%), O (30.2%)
Calcite	2	CaCO <sub>3</sub>	Ca (40%), C (12%), O (48%)
Quartz	3	SiO <sub>2</sub>	Si (48%), O (53%)
Water	4	H <sub>2</sub> O	H (11.2%), O (88.8%)
Cellulose (organic)	5	C <sub>6</sub> H <sub>10</sub> O <sub>5</sub>	C (44.5%), H (6.2%), O (49.3%)

**Fig. 2** Sketch of the transmission experiment. During the transmission experiment, the sediment sample is on top of the detector end cap and the point source is 10 cm above the detector end-cap sustained by a plastic holder with a hole in the center

set of effective activity ratios  $r_{\text{effec}_k}$ . If the activity ratios are not close to unity, see Fig. 1, the algorithm produces a random vector  $\Delta \mathbf{w}$  which will be added to the component vector  $\mathbf{w}$  and will repeat the activity ratios calculation. The process will be repeated iteratively until the value of  $\chi^2$  will be minimized. Finished calculations, the algorithm will produce an output vector  $\mathbf{w}_{\text{final}}$  with values of the effective composition for the sediment sample, see Fig. 3. Detailed information about the model can be obtained in “Appendix” of this work: Algorithm description.

## Experimental procedure

### Gamma spectrometry

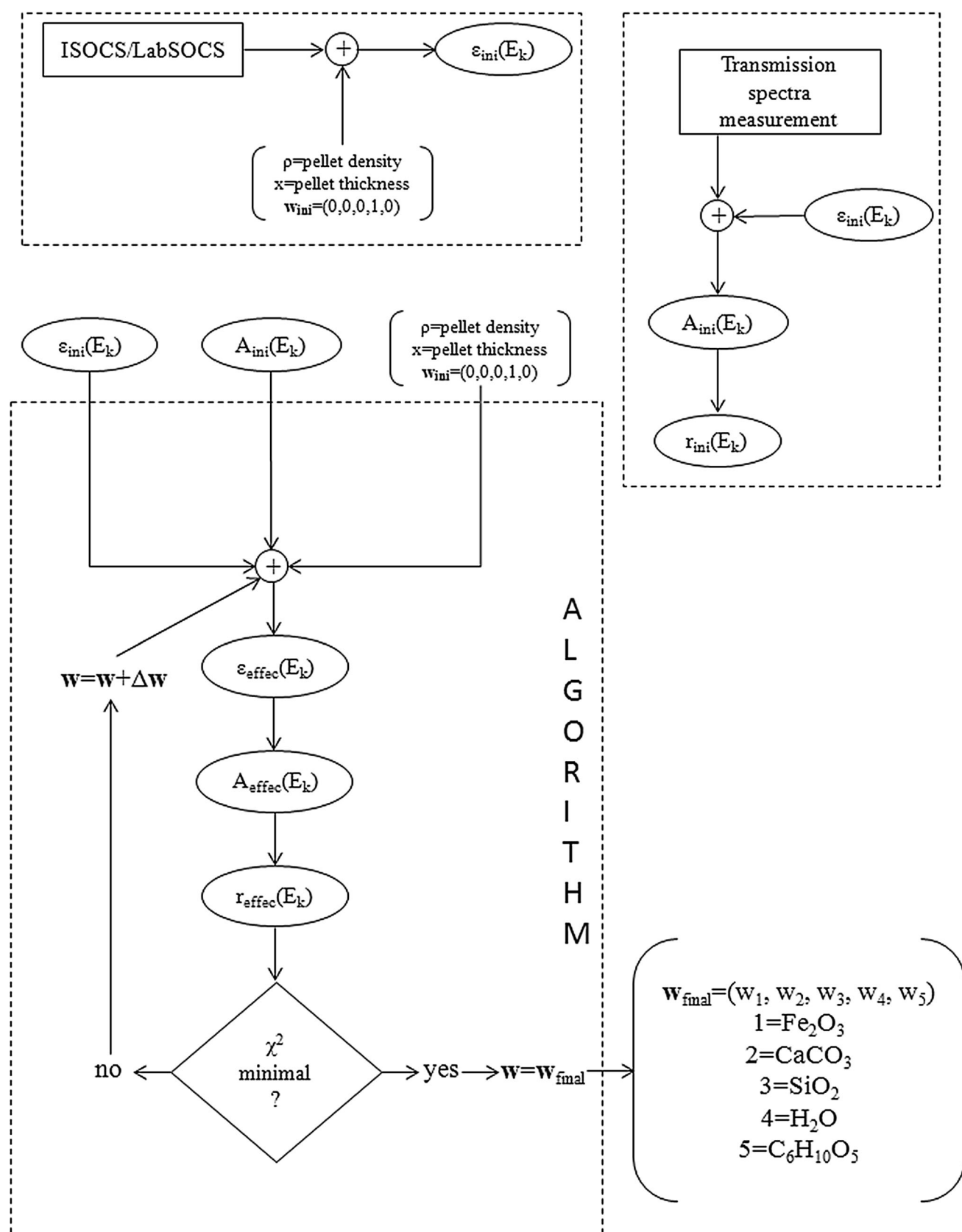
Measurements were performed with a reverse electrode coaxial HPGe detector (Canberra Industries, 50% rel. efficiency), with Cu end cap and carbon window. The detector is housed in a 10 cm Pb shielding followed by a Cu, Cd and plastic inner layer. Spectra were analyzed using Genie 2000 software. Reference efficiency calibrations for the configuration detector-absorber-source were obtained using the Geometry Composer tool from Genie 2000 software. The point source used was a  $^{155}\text{Eu}/^{22}\text{Na}$  source encapsulated in acrylic plastic disc. The certified activity for the isotope  $^{155}\text{Eu}$  was  $(37.0 \pm 7.4)$  kBq on 25th February 2004.

### Test material

Validation of the procedure was done using two reference materials: IAEA-384 and IAEA-385. Sample IAEA-384 is a sediment collected from the Fangataufa Lagoon in French Polynesia. The sample is presented as dry sediment, sieved at 250  $\mu\text{m}$  and homogenized. Sediment composition is considered to be 100% CaCO<sub>3</sub>, with a dry density of  $(2.64 \pm 0.06)$  g cm<sup>-3</sup> [15]. Sample IAEA-385 is a sediment from the Irish Sea. The sample is mainly composed of Si (160 mg g<sup>-1</sup>), Ca (55 mg g<sup>-1</sup>), Al (45 mg g<sup>-1</sup>), Fe (31 mg g<sup>-1</sup>) and K (18 mg g<sup>-1</sup>). The total carbon content is 2.75% and nitrogen 0.13% [16]. The rest of the composition until 100% in this work is considered oxygen.

The material was formed into cylindrical pellets of 70 mm diameter. Both samples were introduced into a hydraulic press applying 26 MPa pressure during 60 s. Measuring the individual thickness, the bulk density was calculated, see Table 2.

After pressing, pellets were sealed in radon-tight aluminum barrier foil. The foil consists of three layers compound foil of 12  $\mu\text{m}$  polyethylene terephthalate, 12  $\mu\text{m}$  Al and 95  $\mu\text{m}$  low-density polyethylene with the objective to obtain secular equilibrium between radon and the daughter products. This was necessary to obtain decay corrected values of  $^{210}\text{Pb}$  via separation of the supported and



◀**Fig. 3** Flow diagram of the method explained in three main blocks. First a reference efficiency created by LabSOCS/ISOCS is provided, in this case water has been chosen as initial material composition. Secondly, using the initial composition, activities can be calculated from the transmission spectra. Finally, using the results from the last blocks as input for the algorithm, the effective composition vector is produced as output after minimize the  $\chi^2$  value

**Table 2** Experimental values of thickness and density calculated for samples IAEA-384 and IAEA-385

Sample	Thickness (mm)	Mass (g)	Density (g cm <sup>-3</sup> )
IAEA-384	7.6 ± 0.1	48.10 ± 0.01	1.64 ± 0.02
IAEA-384	6.4 ± 0.1	43.90 ± 0.01	1.78 ± 0.03

unsupported <sup>210</sup>Pb. Sediments were stored during almost 1 month waiting for the cited equilibrium.

### Transmission experiment

For both samples, individual gamma measurements were done during ca. 24 h. These measurements were used firstly as background spectra during the transmission analysis and later on as measurements for multi-nuclide quantification after efficiency calibration. Samples were placed centered on the carbon window. The point source was placed on a holder (10.0 ± 0.1) cm above the detector end cap, see Fig. 1. Spectra were recorded for the transmission geometry until the uncertainty for the 45.3 keV ( $I = 1.31 \pm 0.05\%$ ) peak was under 2%.

Taking into account the detector-absorber-source configuration, initial FEPEs using the Geometry composer tool from Genie 2000 software were created especially for the energies of gamma and X-rays from the <sup>155</sup>Eu isotope. Lines used in the algorithm can be found in Table 3.

The point source was modeled as a point of 0.1 mm<sup>3</sup> active volume in the middle of an acrylic plastic disc (Methyl methacrylate) with a diameter of 25 mm and a thickness of 6 mm. Samples were modeled as a disc with dimensions and density determined by measurements, see Table 2. Cascade correction was done, taking into account

the geometry, with Genie 2000 software. It can be observed that due to geometry, cascade summing effects are negligible, see Table 3.

## Results and discussion

Following the presented methodology, activity ratios from transmission experiments were calculated, see Figs. 4 and 5. Activity ratios for both samples show how a wrong choice of the samples chemical composition (water) can produce a discrepancy from unity in ratios. In the case of the certified composition, ratios are close to unity allowing calculation of the activity of the point source whatever line was chosen. The composition is not necessary identical to the certified one, it can be expected that not only one chemical mixture can reproduce the real self-absorption in the sample. Effective composition result shows how a compound mixture generated by the method can produce ratios close to unity, see Table 4.

Mass attenuation coefficients produced by the method [see “Appendix”: Eq. (3)] are presented in Figs. 6 and 7. In sample IAEA-384 it can be observed, when the certified composition is chosen, mass attenuation coefficient produced does not disagree with the effective one, see Fig. 6. It reinforces the idea that an effective composition can play the same role as the real one in photon absorption. In the case of the sample IAEA-385, certified composition and effective one do not produce the same activity ratio values, (see Fig. 7) but values which are inside of the uncertainty range, see Fig. 5. The mass attenuation coefficients for certified and effective mixture used for IAEA-385 show clearly differences that explain the activity ratios difference, see Fig. 7.

In order to check the reliability of Eq. (3) (see “Appendix”), individual values of  $\mu$  for the selected chemical composition (water, certified composition and effective) were extracted from the XCOM database [18] and plotted together with values produced by Eq. (3), showing that the model produces a good agreement in the mass attenuation coefficient calculations, see Figs. 6 and 7.

**Table 3** Used photons lines of <sup>155</sup>Eu together with emission probability, photon type, cascade summing correction and model index  $k$ , for the source-absorber-detector geometry (see Fig. 1) performed by Genie 2000 software used for the transmission spectra [17]

Algorithm index $k$	Energy (keV)	Intensity (%)	Type	Cascade correction
1	43.00	12.1 ± 0.2	$X_{K\alpha 1}$	1.000
2	48.77	3.8 ± 0.1	$X_{K\beta 1}$	1.000
3	60.01	1.22 ± 0.05	$\gamma$	0.999
4	86.55	30.7 ± 0.3	$\gamma$	Free
5	105.31	21.1 ± 0.6	$\gamma$	1.000
6	146.07	0.051 ± 0.004	$\gamma$	1.000

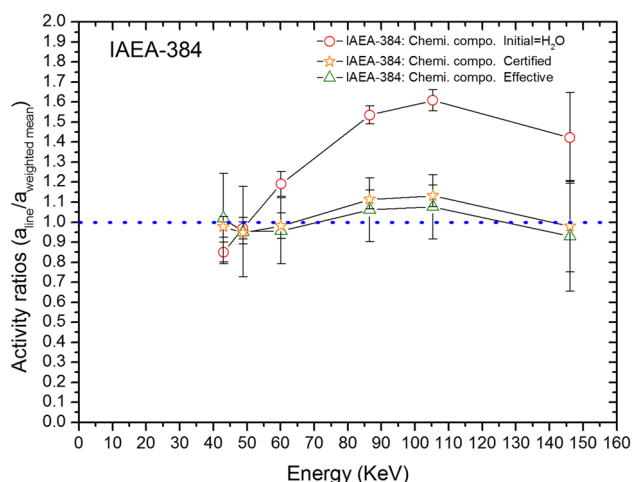


**Fig. 4** Activity ratios calculated for the transmission experiment using a  $^{155}\text{Eu}$  point source and samples compositions: initial:  $\text{H}_2\text{O}$ , certified composition: 100%  $\text{CaCO}_3$  and effective composition by the method for the IAEA-384 sample

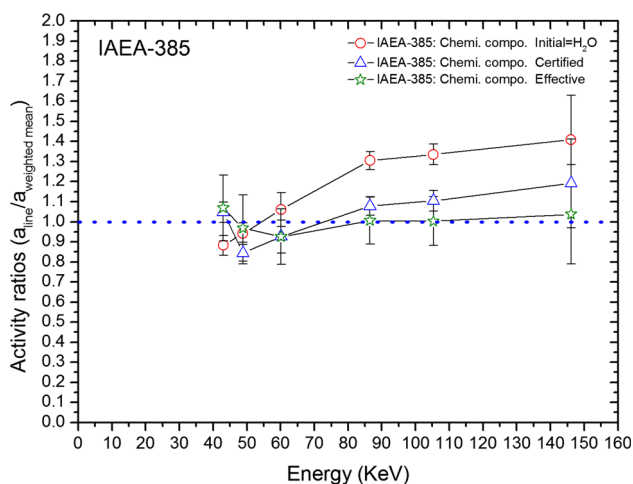


**Fig. 5** Activity ratios for the transmission experiment using a  $^{155}\text{Eu}$  point source and samples compositions: initial:  $\text{H}_2\text{O}$ , certified composition and effective composition by the proposed method for the IAEA-385 sample

FEPE produced by LabSOCS for the transmission experiment using the chemical compositions from the previous step can be found in Figs. 8 and 9. Disagreement is expected for the wrong choice of absorber material, e.g.: water, for both cases. Agreement between the FEPEs generated for cases with the certified composition and effective composition for sample IAEA-384 can be found, see Fig. 8. Sample IAEA-385 presents disagreement in the FEPE calculated for the certified and effective composition, see Fig. 9. It is observed again as well as in Figs. 5 and 7. The cause for the difference is most probably the deviation from the chemical composition certified [16].

Once FEPEs are determined for transmission experiment, activities for the point source can be calculated, see

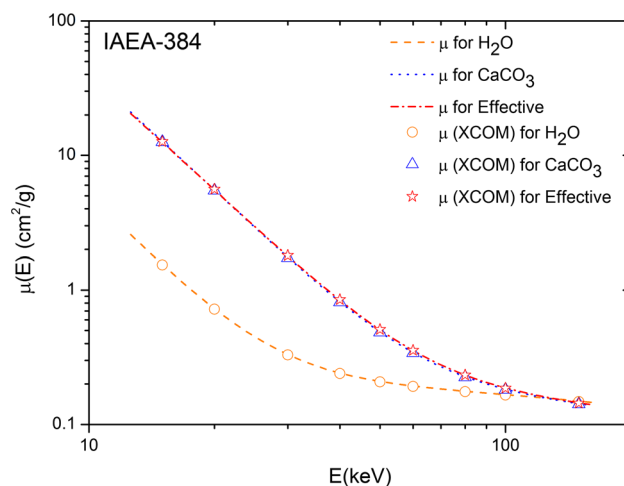


**Fig. 6** Mass attenuation coefficients for: water, certified composition (IAEA-384: 100%  $\text{CaCO}_3$ ) and effective composition, see Table 4. Values of XCOM database have been plotted together to test the reliability of the  $\mu$  calculation

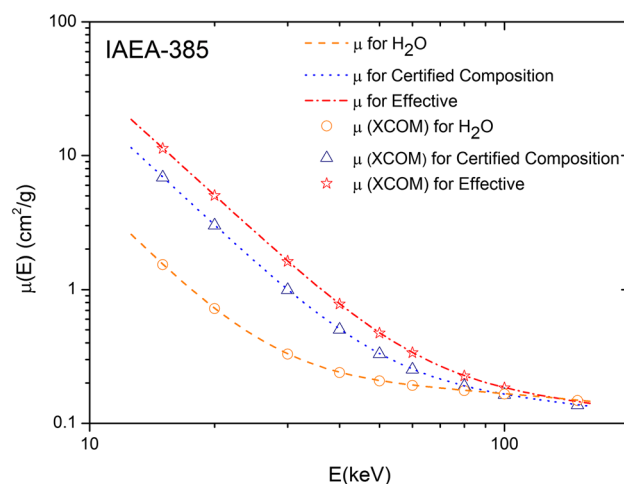


**Fig. 7** Mass attenuation coefficients for: water, certified composition (IAEA-385: C: 2.75% N: 0.13% Al: 4.5% Si: 16% K: 1.8% Ca: 5.5% Fe: 3.1% O: 66.22%) and effective composition, see Table 4. Values of XCOM database have been plotted together to test the reliability of the  $\mu$  calculation

Figs. 10 and 11. Comparing activities obtained for certified and optimized composition shows that both compositions model the absorber with a good agreement. In the case of using a wrong absorber e.g.: water, activities disagree as expected in the range of low energy. Due to the  $\pm 20\%$  uncertainty in the certified activity from the point source, (irrelevant for the iterative process, as only activity ratios are considered and optimized) a comparison between measurements of the transmission experiment with a measurement from the point source without absorber have been done. In that case, FEPE produced by LabSOCS/ISOCS for a point source within an acrylic plastic disc, geometrical configuration as described in the transmission



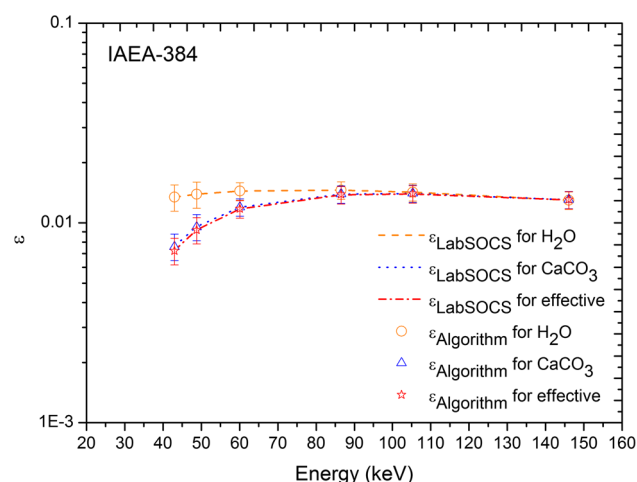


**Fig. 8** Efficiency curves used for sample IAEA-384. Efficiencies produced by the proposed method were plotted together with efficiencies from LabSOCS/ISOCS

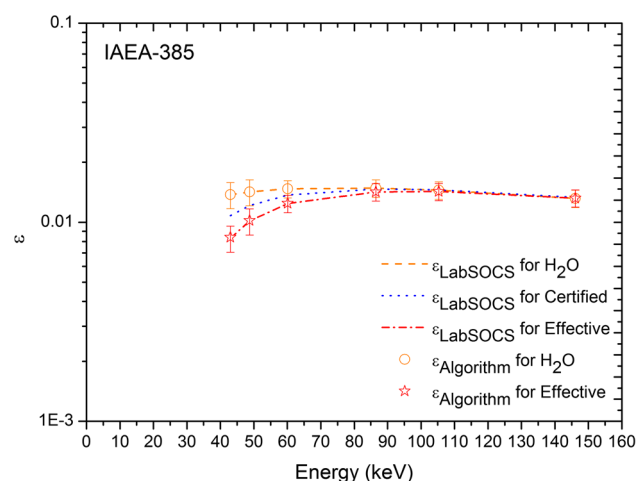


**Fig. 9** Efficiency curves for sample IAEA-385. Efficiencies produced by the proposed method were plotted together with efficiencies from LabSOCS/ISOCS. Here, only efficiencies produced by LabSOCS/ISOCS with water and effective composition are shown

experiment paragraph and only the line of 86.5 keV (see, Table 3) with no cascade corrections was considered. This way, an activity value for  $^{155}\text{Eu}$  of  $(6.29 \pm 0.26)^1$  kBq on to 3rd March 2017 for a measurement with no absorber was calculated. Looking at Fig. 11 for the sample IAEA-385 again differences in the low energy range for certified composition and effective ones are obtained. Comparing activities from the measurement where the point source is present without absorber, (see Figs. 10, 11 dashed line) activities calculated with effective composition are closer to the activity of the punctual source. It appears to reinforce the idea that the certified composition for sample IAEA-385 may omit some elements.

<sup>1</sup> The activity has been calculated within one sigma deviation.

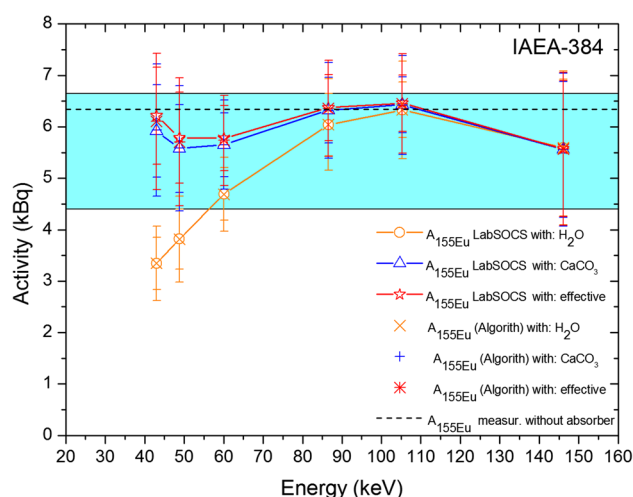


**Fig. 10** Activities for the point source calculated from transmission experiment using as absorber the sample IAEA-384. Activity values for the  $^{155}\text{Eu}$  lines are calculated using compositions by LabSOCS and by the algorithm. In dashed line experimental activity measured from  $^{155}\text{Eu}/^{22}\text{Na}$  point source without absorber. In blue box the certified values range from the  $^{155}\text{Eu}/^{22}\text{Na}$  point source. All activities are calculated on 3rd March 2017. (Color figure online)

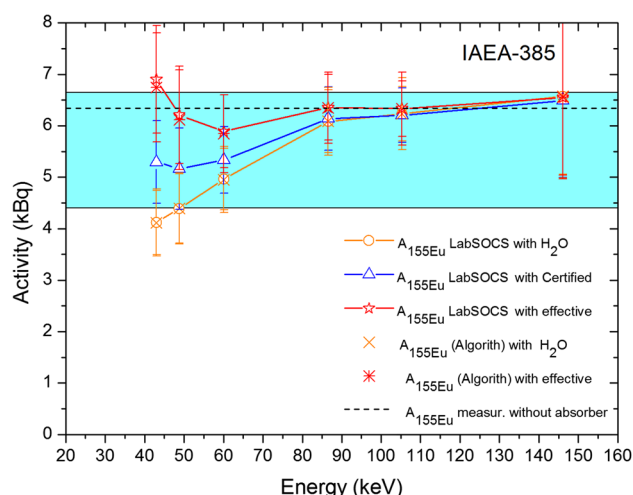


**Fig. 11** Activities for the point source during transmission experiment. Values for the  $^{155}\text{Eu}$  lines are calculated using LabSOCS and the algorithm here proposed. In dashed line experimental activity measured from  $^{155}\text{Eu}/^{22}\text{Na}$  point source without absorber. In blue box the certified values range from the  $^{155}\text{Eu}/^{22}\text{Na}$  point source. All activities are calculated on 3rd March 2017. (Color figure online)

Finally, compositions (certified and effective) were used to produce new FEPEs in a detector-source geometrical configuration. Both sediment samples were modeled as in the transmission experiment, just without point source. Results from certified activities from both samples IAEA-384 and IAEA-385 were compared with results<sup>2</sup> from the

<sup>2</sup> The uncertainty of the activities in this work has been given as one sigma deviation.

**Table 4** Effective chemical composition, in percent for samples IAEA-384 and IAEA-385, determined by the algorithm

Mineral	Composition	IAEA-384 (%)	IAEA-385 (%)
Hematite	Fe <sub>2</sub> O <sub>3</sub>	18	15
Calcite	CaCO <sub>3</sub>	24	33
Quartz	SiO <sub>2</sub>	32	12
Water	H <sub>2</sub> O	0	0
Cellulose (organic)	C <sub>6</sub> H <sub>10</sub> O <sub>5</sub>	26	40

**Table 5** Experimental activity concentrations for the reference sample IAEA-384, compared with certified values

Nuclide/line used	Certified value/95% conf. interval (Bq kg <sup>-1</sup> )	Values for IAEA-384 (Bq kg <sup>-1</sup> )	
		FEPE “certified composition”	FEPE “effective composition”
<sup>155</sup> Eu (86.55 keV)	7.0/(6.7–7.3)	7.94 ± 2.28	7.98 ± 2.29
<sup>241</sup> Am (59.54 keV)	7.1/(6.7–7.4)	7.80 ± 1.19	7.90 ± 1.21
<sup>210</sup> Pb (46.54 keV) <sup>a</sup>	22/(21–23)	20.9 ± 5.1	21.4 ± 5.2
<sup>226</sup> Ra (351.93 keV)	2.4/(2.0–2.9)	1.92 ± 0.29	1.91 ± 0.28

Calculations have been done for the certified and effective compositions of the sample. Activities are referred to 1 August 1996

<sup>a</sup><sup>210</sup>Pb here shown is total, composed of supported and unsupported fraction. Calculations have been done, first getting the unsupported part by subtraction from the total:  $^{210}\text{Pb}_{\text{xs}} = ^{210}\text{Pb}_{\text{total}} - ^{210}\text{Pb}_{\text{supp}} (^{226}\text{Ra})$ . Second, correcting by radioactive decay only the  $^{210}\text{Pb}_{\text{xs}}$  part, and finally that part has been added to the supported contribution  $^{210}\text{Pb}_{\text{supp}}$  thus obtaining the total  $^{210}\text{Pb}$  corrected to time of issue of the certificate

**Table 6** Experimental activity concentrations for the reference sample IAEA-385, compared with certified values

Nuclide/line used	Certified value/95% conf. interval (Bq kg <sup>-1</sup> )	Values for IAEA-385 (Bq kg <sup>-1</sup> )	
		FEPE “certified composition”	FEPE “effective composition”
<sup>241</sup> Am (59.54 keV)	3.84/(3.78–4.01)	3.38 ± 0.54	3.61 ± 0.58
<sup>210</sup> Pb (46.54 keV)	32.9/(31.2–35.3)	32 ± 12	40 ± 14
<sup>226</sup> Ra (351.93 keV)	21.9/(21.6–22.4)	22.24 ± 2.18	22.28 ± 2.19

Calculations expressed for certified and effective compositions. Decay correction referred to 1 January 1996

gamma analysis in case where the FEPE was calculated with certified composition and with effective one for both samples. All measurements were corrected with the decay correction for the corresponding sample [15, 16], except the <sup>226</sup>Ra which was measured via secular equilibrium within <sup>214</sup>Pb (351.9 keV), after decay of <sup>222</sup>Rn, see Tables 5 and 6.

## Conclusions

In the present work, activities concentration of natural and artificial radionuclides of low gamma energy emission in two sediment samples with certified activities and chemical

composition have been experimentally measured and compared. Transmission measurements within <sup>155</sup>Eu point source have been done producing activity ratio plots. Using the method here developed, effective chemical composition have been produced and implemented in LabSOCS/ISOCS to produce efficiency curves. Finally, activities concentrations in sediment have been calculated. Activity concentrations in all cases are within its uncertainty in the range of the certified value. Special mention is the high uncertainty for <sup>210</sup>Pb, which due to decay correction of one of its component, get an increase of the uncertainty. We conclude that the method proposed can be a quick solution for self-absorption correction of low energy gamma isotopes in sediment samples with unknown composition. The algorithm can be developed easily in one spreadsheet staying open to be used with different sample compositions. Using only one point source with a multi-energetic isotope in the energy range of interest, costs and experimental time during the transmission experiment can be reduced.

**Acknowledgements** Acknowledgments are especially to (Postgraduate International Programme) PiP for the financial support and to the student Dennis Schmidt who tested the method during his Bachelor thesis.



## Appendix: Algorithm description

The effective mass attenuation coefficient  $(\mu/\rho)_{\text{effec}}$  represents the photon absorption in the sediment sample and can be written as a compound from individual mineral compositions. It can be expressed by

$$\left(\frac{\mu}{\rho}\right)_{\text{effec}} = \sum_{i=1}^5 w_i \left(\frac{\mu}{\rho}\right)_i \quad (2)$$

where  $(\mu/\rho)_i$  represent the mass attenuation coefficient of the  $i$ th material from the Table 1 and  $w_i$  is the weight fraction of the  $i$ th material [14, 19]. Due to the fact that the sediment chemical composition in function of five basic compounds listed in Table 1 needs to be expressed, coefficient  $w_i$  has five degrees of freedom from our model. Elements can be reduced in the case, where it is known that compounds (e.g. water) are not present in the sample. Equation (2) is rewritten as a function of the energy using ten empirically determined coefficients  $j$  per compound  $i$  introduced in a sum of exponential functions [20]

$$\left(\frac{\mu(E, w_i)}{\rho}\right)_{\text{effec}} = \sum_{i=1}^5 w_i \cdot \exp\left(\sum_{j=0}^9 x_{ij} \cdot (\ln(E))^j\right) \quad (3)$$

where empirical coefficients  $x_{ij}$  are for every compound  $i$  from the Table 1 used in this work, calculated and stored in the library by the program ISOCS/LabSOCS (see in supplementary information).

Thenceforth, the non-attenuation corrected detection FEPE at the selected energies can be calculated using the inverted classical formula:

$$\varepsilon_0(E_k) = \varepsilon_{\text{ini}}(E_k) \cdot \exp\left(\left(\frac{\mu(E_k)}{\rho}\right)_{\text{ini}} \cdot \rho x\right) \quad (4)$$

[20], where  $\left(\frac{\mu(E_k)}{\rho}\right)_{\text{ini}}$  is the mass attenuation coefficient for the initial material used for the initial values of FEPE, in our example: water 100% and  $\rho x$  is the average sample mass per unit of area. Efficiencies for an effective composition can be calculated using the last results.

$$\varepsilon_{\text{effec}}(E_k, w_i) = \varepsilon_0(E_i) \cdot \exp\left(-\left(\frac{\mu(E_k, w_i)}{\rho}\right)_{\text{effec}} \cdot \rho x\right) \quad (5)$$

In practical situations Eqs. (4) and (5) can be written in a compact formula with input  $w_i$  as variable parameters and output the new FEPEs for an effective material:

$$\begin{aligned} \varepsilon_{\text{effec}}(E_k) &= \varepsilon_{\text{effec}}(\varepsilon_{\text{ini}}(E_k), w_i, \rho x) \\ &= \varepsilon_{\text{ini}}(E_k) \\ &\quad \cdot \exp\left(-\left\{\left(\frac{\mu(E_k, w_i)}{\rho}\right)_{\text{effec}} - \left(\frac{\mu(E_k)}{\rho}\right)_{\text{ini}}\right\} \cdot \rho x\right) \end{aligned} \quad (6)$$

FEPEs calculated are a computational result, activity ratios calculated for the lines of  $^{155}\text{Eu}$  need to be used. Efficiencies can be connected with activity ratios via activity values. To do that, activities calculated for the initial material, following the example: water 100% is used. Activity of every line from the  $^{155}\text{Eu}$  can be calculated with the well know formula [14, 21]

$$A_{\text{ini}_k} = \frac{N - B}{t_l \cdot \varepsilon_{\text{ini}}(E_k) \cdot I} \quad (7)$$

where  $N$  is the number of counts in the peak of energy  $E_k$  for the transmission measurement,  $B$  is the number of background counts at energy  $E_k$ ,  $t_l$  is the measured live time for the transmission measurement,  $\varepsilon_{\text{ini}}(E_k)$  is the FEPE for initial material and  $I$  is the photon emission probability.

Changes of chemical composition in the sample are computerized by variation of the vector  $\mathbf{w}$  in the algorithm. It produces new activities  $A_{\text{effec}_k}$  as a result of variations of  $\mu_{\text{effec}}$  and consequently  $\varepsilon_{\text{effec}}(E_k)$  via Eqs. (3 and 6). As well as in Eq. (7), for effective material activities can be calculated using

$$A_{\text{effec}_k} = \frac{N - B}{t_l \cdot \varepsilon_{\text{effec}}(E_k) \cdot I} \quad (8)$$

where all parameters from Eq. (8) will stay constant for computational changes in the chemical composition except  $\varepsilon_{\text{effec}}(E_k)$ . Taking into consideration the last sentence, effective activities  $A_{\text{effec}_k}$  calculated during the execute of the algorithm, can be calculated from Eq. (7) and Eq. (8) via  $\varepsilon_{\text{effec}}(E_k)$  with

$$A_{\text{effec}_k} = \frac{\varepsilon_{\text{ini}}(E_k)}{\varepsilon_{\text{effec}}(E_k)} A_{\text{ini}_k} \quad (9)$$

Effective activities for the transmission experiment can be calculated by changing the input parameters  $w_i$  in the algorithm. Activity ratios are nevertheless magnitudes dependent from the activity of the point source, for this reason, activities ratios will be the magnitude used in the next steps.

Activities ratios  $r_k$  can be calculated as the activity of every line divided by the activity calculated for a reference line or key line. An alternative and more general definition in case where the radioisotope presents not a predominant line but in case when it has several lines with similar emission probability is to calculate the activity ratio as the activity of every line divided by the weighted average activity calculated from all identified lines of the nuclide. It can be expressed as

$$r_k = \frac{A_k}{A_{wm}} \quad (10)$$

from Eq. (10) the weighted average activity  $A_{wm}$  can be calculated as

$$A_{wm} = \frac{\sum_{k=1}^N \frac{A_k}{\sigma_{A_k}^2}}{\sum_{k=1}^N \frac{1}{\sigma_{A_k}^2}} \quad (11)$$

where  $A_k$  represents the activity calculated for every  $k$  line of the identified nuclide and  $\sigma_{A_k}$  is the standard deviation of activity  $A_k$  calculated from all parameters included in Eq. (7) [20] and  $N$  is the number of lines identified in the transmission spectra, see Table 3. Equation (11) weighs every  $k$  line result with its standard deviation. Thus, in cases where lines with high uncertainty are present, the mean value is little affected. In cases of one nuclide<sup>3</sup> with only one predominant line Eq. (11) is reduced to the activity calculated with the key line.

Taking into account Eqs. (10) and (11), ratios for the initial material necessary as input for start the algorithm can be calculated using

$$r_{ini_k} = \frac{A_{ini_k}}{\sum_{k=1}^N \frac{A_{ini_k}}{\sigma_{A_{ini_k}}^2}} \quad (12)$$

and as extension from Eq. (12) activity ratios for changes of the material composition in the sample during the running of the algorithm can be written as

$$r_{effec_k} = \frac{A_{effec_k}}{\sum_{k=1}^N \frac{A_{effec_k}}{\sigma_{A_{effec_k}}^2}} \quad (13)$$

where we need to remember that  $A_{effec_k}$  for the  $k$  line are calculated using Eq. (9) and the standard deviation  $\sigma_{A_{effec_k}}$  is calculated using the error propagation formula. The uncertainty can be calculated as

$$\sigma_{A_{effec_k}} = A_{effec_k} \sqrt{\left(\frac{\sigma_{\varepsilon_{effec_k}}}{\varepsilon_{effec_k}}\right)^2 + \left(\frac{\sigma_{\varepsilon_{ini_k}}}{\varepsilon_{ini_k}}\right)^2 + \left(\frac{\sigma_{A_{ini_k}}}{A_{ini_k}}\right)^2} \quad (14)$$

For Eq. (14)  $A_{ini_k}$ ,  $\sigma_{A_{ini_k}}$  and  $\varepsilon_{ini_k}$  are taken from the initial analysis or “initial analysis” used as input for the algorithm and  $\sigma_{\varepsilon_{effec_k}}$  as well as  $\sigma_{\varepsilon_{ref_k}}$  are calculated as the fixed percent of the FEPE expressed by the software manufacturer and cited in the introduction of this work [12].

Concluding in Eq. (13), effective activity ratio curves can be produced just adjusting the free parameters  $w_i$ . As a consequence, usable composition is reached when effective activity ratios values close unity as shown in, see Figs. 4 and 5.

The procedure employed in this work to find the optimal effective composition consists of minimizing the global  $\chi^2$ . It is defined as

$$\chi^2 = \left[ \sum_{k=E_i}^{E_f} |r_{effec_k} - 1| \right]^2 \quad (15)$$

where  $k$  indicates every individual line from the isotope  $^{155}\text{Eu}$ . The parameter can be easily minimized using an iterative process where initially the vector  $\mathbf{w} = (w_1, w_2, w_3, w_4, w_5)$  with a set of elements  $w_i$  of every material from the Table 1 is used to calculate the  $\chi$  value. If the value of the  $\chi^2$  is not minimal, the algorithm repeats the calculation changing the elements of the vector as  $\mathbf{w} + \Delta\mathbf{w}$ , where  $\Delta\mathbf{w}$  is a vector with random components  $\Delta\mathbf{w}_i$   $i = (1, 2, 3, 4, 5)$ . The algorithm is finished when minimal value of  $\chi^2$  is reached, see Fig. 3.

In the present work, the algorithmic has been implemented in a excel sheet. Together with the excel solver tool, the  $\chi$  parameter has been minimized taking into account five parameters  $w_i$ . The number of interactions has been established in 1000 with a tolerance level of 1%.

From Eq. (15) the same number of  $k$  lines detected from the  $^{155}\text{Eu}$  source and quantified in the transmission spectra need to be considered. Minimization of  $\chi^2$  needs to be carried out taking into account in every execution: (A) the sum of the coefficients  $w_i$  is one:

$$\sum_{i=1}^5 w_i = 1. \quad (16)$$

From Eq. (16) it can be understood that the sum of all percentages from the composition involved in Table 1 need to be normalized. Where  $i$ th indicates:  $i = 1 = \text{Fe}_2\text{O}_3$ ;  $i = 2 = \text{CaCO}_3$ ; etc., see Fig. 3. (B) Every weight fraction of the  $i$ th element  $w_i$  is limited in the upper value to one and in the lower to zero. It can be expressed as

$$0 \leq w_i \leq 1 \quad (17)$$

From Eq. (17) it can be understood that the algorithm can reduce the number of degree of freedom in case where it would be necessary.<sup>4</sup>

<sup>3</sup> It is not necessary to use  $^{155}\text{Eu}$ . Alternatively, a different radionuclide with several energy lines concentration in the energy range of interest can be used.

<sup>4</sup> Additionally, the number of compositions can be reduced by setting  $w_i$  to zero in case where information about the sample composition is provided. E.g:  $w_{\text{H}_2\text{O}} = 0$  for dry sediments.

## References

1. Appleby PG (2008) Three decades of dating recent sediments by fallout radionuclides: a review. *The Holocene* 18(1):83–93
2. Appleby PG et al (1991)  $^{241}\text{Am}$  dating of lake sediments. *Hydrobiologia* 214(1):35–42
3. O'Reilly J et al (2010)  $^{210}\text{Pb}$ -dating of a lake sediment core from Lough Carra (Co. Mayo, western Ireland): Use of paleolimnological data for chronology validation below the  $^{210}\text{Pb}$  dating horizon, vol 102. <https://doi.org/10.1016/j.jenvrad.2010.09.003>
4. Perez-Moreno JP et al (2002) A comprehensive calibration method of Ge detectors for low-level gamma-spectrometry measurements. *Nucl Instrum Methods A* 491(1–2):152–162
5. Schuler C et al (1991) A multitracer study of radionuclides in Lake Zurich, Switzerland: 1. Comparison of atmospheric and sedimentary fluxes of  $^7\text{Be}$ ,  $^{10}\text{Be}$ ,  $^{210}\text{Pb}$ ,  $^{210}\text{Po}$ , and  $^{137}\text{Cs}$ . *J Geophys Res* 96(C9):17051
6. Hurtado S et al (2007) A self-sufficient and general method for self-absorption correction in gamma-ray spectrometry using GEANT4. *Nucl Instrum Methods Phys Res* 580(1 SPEC. ISS.):234–237
7. Cutshall NH et al (1983) Direct analysis of  $^{210}\text{Pb}$  in sediment samples: self-absorption corrections. *Nucl Instrum Methods Phys Res* 206(1):309–312
8. Joshi SR (1989) Determination of  $^{241}\text{Am}$  in sediments by direct counting of low-energy photons. *Int J Radiat Appl Instrum* 40(8):691–699
9. Overwater RMW et al (1993) Gamma-ray spectroscopy of voluminous sources Corrections for source geometry and self-attenuation. *Nucl Instrum Methods Phys Res* 324(1):209–218
10. García-Talavera M et al (2004) A hybrid method to compute accurate efficiencies for volume samples in  $\gamma$ -ray spectrometry. *Appl Radiat Isot* 60(2–4):227–232
11. Hurtado S (2014) IAEA seminar: gamma spectrometry and quality management: Autoabsorption, vol A3. Santo Domingo, Dominican Republic
12. Technologies M (2012) Technical advantages of ISOCS<sup>TM</sup>/Lab-SOCS<sup>TM</sup>. [http://www.canberra.com/literature/isocs/application\\_notes/ISOCS-LabSOCS-App-Note-C39530.pdf](http://www.canberra.com/literature/isocs/application_notes/ISOCS-LabSOCS-App-Note-C39530.pdf). Accessed 5 May 2017
13. Pittauerová D et al (2009) Application of self-absorption correction method in gamma spectroscopy for  $^{210}\text{Pb}$  and  $^{137}\text{Cs}$  sediment chronology on the continental slope off NW Africa. *Radioprotection* 44(5):457–461
14. Debertin K et al (1988) Gamma- and X-ray spectrometry with semiconductors detectors. North-Holland, Amsterdam
15. Povinec PP et al (2007) Reference material for radionuclides in sediment IAEA-384 (Fangataufa Lagoon sediment). *J Radioanal Nucl Chem* 273(2):383–393
16. Pham MK et al (2008) A new certified reference material for radionuclides in Irish sea sediment (IAEA-385). *Appl Radiat Isot* 66(11):1711–1717
17. Becquerel LNH (2015) Mini Table de radionucléides 2015. EDP Sciences
18. Berger MJ et al (1999) XCOM: photon cross section database, v1.2. National Institute of Standards and Technology, Gaithersburg, MD. <http://physics.nist.gov/xcom>
19. Nelson G et al (1991) Passive nondestructive analysis of nuclear materials. In: laboratory Lan (ed) Gamma-ray interactions with matter, pp 27–42
20. Canberra I (2006) Genie<sup>TM</sup> 2000 3.1 Customization Tools Manual
21. Knoll GF (2010) Radiation detection and measurement. Wiley, Hoboken